Surface Coverage in Wireless Sensor Networks

Ming-Chen Zhao, Jiayin Lei, Min-You Wu
Shanghai Jiao Tong University
China

Yunhuai Liu
Hong Kong Univrsity of
Science and Technology, China

Wei Shu
The University of
New Mexico, USA

***Abstract*—Coverage is a fundamental problem in Wireless Sensor Networks (WSNs). Existing studies on this topic focus on 2D ideal plane coverage and 3D full space coverage. The 3D surface of a targeted Field of Interest is complex in many real world applications; and yet, existing studies on coverage do not produce practical results. In this paper, we propose a new coverage model called *surface coverage*. In surface coverage, the targeted Field of Interest is a complex surface in 3D space and sensors can be deployed only on the surface. We show that existing 2D plane coverage is merely a special case of surface coverage. Simulations point out that existing sensor deployment schemes for a 2D plane cannot be directly applied to surface coverage cases. In this paper, we target two problems assuming cases of surface coverage to be true. One, under stochastic deployment, how many sensors are needed to reach a certain expected coverage ratio? Two, if sensor deployment can be planned, what is the optimal deployment strategy with guaranteed full coverage with the least number of sensors? We show that the latter problem is NP-complete and propose three approximation algorithms. We further prove that these algorithms have a provable approximation ratio. We also conduct comprehensive simulations to evaluate the performance of the proposed algorithms.**

I. Introduction

Coverage is a fundamental problem in Wireless Sensor Networks (WSNs). Each sensor is designed and deployed with the central task of sensing a section of a Field of Interest (FoI). A FoI is considered fully covered if and only if every point on the surface is covered by at least one sensor. The quintessence of the coverage problem is to use the least number of sensors to satisfy specific service requirements, e.g. coverage ratio, network connectivity and robustness. Solutions to the coverage problem have important applications in base station deployment in cellular networks, coverage in wireless mesh networks, etc.

Existing work on coverage issues focus mainly on 2D plane coverage or 3D full space coverage. In 2D plane coverage [1] [2], sensors are only allowed to be deployed on an ideal plane. And, in 3D full space coverage [3] [4], the FoI is assumed to be the 3D full space where sensors can be positioned freely within the whole FoI. In many real world applications, however, the FoI is neither a 2D ideal plane nor a 3D full space. Instead, they are complex surfaces. For example, in the Tungurahua volcano monitoring project [5] (Fig.1(a)), 2D plane coverage solutions do not provide a workable strategy for surface coverage for the volcano, which is a complex surface, without falling victim to the Coverage Hole Problem, as illustrated in Fig.1(b). Similarly, 3D full space coverage solutions cannot be applied either, because sensors in this case can only be deployed on the exposed surface area, and not freely within the volcano. Three-dimensional full space coverage solutions are not discussed in this paper because they differ fundamentally from issues of complex surface coverage.

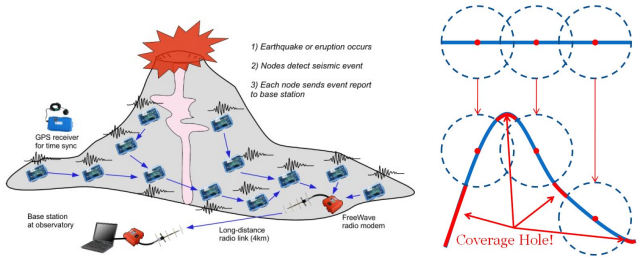

(a) (b)

Fig. 1. A complex sensor coverage; a). A case study of volcano monitoring project by Harvard Sensor Networks Lab [5]; b). Coverage problem by directly applying a traditional method.

In response to the need for a coverage solution for complex surfaces, we propose an innovative coverage model called surface coverage. We present surface coverage as a solution to coverage problems in WSNs (complex surfaces) that is superior to solutions derived from traditional 2D ideal plane and 3D full space coverage methodologies. Nonetheless, the advantages of surface coverage come with new challenges yet to be addressed, e.g., how to handle variations in the shape of the surface. This paper studies two problems in WSN surface coverage. One, the number of sensors that are needed to reach a certain expected coverage ratio under stochastic deployment. Two, the optimal deployment strategy with guaranteed full coverage and the least number of sensors when sensor deployment is pre-determined. We prove that the optimum surface coverage problem is NP-complete when applied to complex surface. Then, we propose three approximation algorithms with a provable performance bound for coverage of complex surfaces. The methodology used in this paper can be extended to other issues in surface coverage, e.g. connectivity problems and mobility problems.

The main results and contributions are summarized as follows:

- To our best knowledge, this work is the first to tackle the problem of surface coverage in WSNs. We propose a new model for the coverage problem.
- We derive analytical expressions of the expected coverage ratio on surface coverage for stochastic deployment. Simulation experiments are conducted to verify the results.

978-1-4244-3513-5/09/$25.00 ©2009 IEEE

- We formalize the planned deployment problem and prove that it is NP-complete. Three approximation algorithms are proposed with provable approximation performance.

The rest of the paper is organized as follows. Related work is summarized in Section II. In Section III, we discuss the basic assumptions and models used throughout the paper. In Section IV, we present the analytical results of the expected coverage ratio under stochastic deployment. In Section V, we describe the solution to the optimum deployment strategy under planned deployment. We evaluate our results in Section VI and discuss some practical issues in Section VII. Section VIII concludes the paper. Due to space limitation, we omitted many proofs and provide only sketches for others.

II. Related Work

There are several ways to classify existing research on the coverage problem. One is the type of FoI: 2D ideal plane FoI [6] [7] [8] [9] [10] [11] [1] [12] [13] [14] [15] [16] [17] [2] or 3D full space FoI [3] [4]. Early work on coverage for the 2D ideal plane assumed that the plane was infinite so as to avoid the edge effect [10] [1] [12] [2], but recent findings have shown these results to be impractical and offer tentative solutions to finite areas [13] [15]. As yet, fundamental problems for these finite areas remain unanswered (e.g. optimum coverage policy and mobile coverage), and coverage solutions for the 2D ideal plane continue to incite heated debate [16] [2]. Still, proposed solutions to the 2D ideal plane problem have found a wide range of applications and some of them are easily applied to the case of 3D full space. All of these results, derived from the 2D plane and then applied to 3D complex surface, suffer from the Coverage Hole Problem.

Another way to classify existing work is by the type of employed sensors. Some early works assumed that sensors were static and homogeneous. More recent work began to consider mobile sensors [10] [16] and heterogeneous sensors [13]. For example, mobile sensors were employed to cover a certain area so that fewer static sensors were needed [10] [16]. Lazos [13] applied a new mathematical tool called "Integral Geometry" to solve the coverage problem when sensors are heterogeneous. Parts of this paper are based on the results from this work [13].

A third way to classify previous research is based on the sensor deployment scheme. A deterministic scheme [12] [2]; that has planned deployment (e.g., manual deployment [18]) needs fewer sensors to cover a given area but is more time-consuming and labor intensive, making it more appropriate for friendly environments. Another deployment scheme is by stochastic or random deployment such as is advocated in [10] [13] [15] [16]. This method deploys sensors by vehicles or air-craft. We consider both these cases.

Also, there is other work that focus on joint optimum goals. Cardei et. al. [11] proposed a scheduling policy to maximize the lifetime of sensor networks. Paper [7] studied the relation between sensing coverage and communication connectivity. And in papers [12] [2], the optimum coverage patterns for an ideal infinite plane with designated connectivity requirements were proposed. In particular, the recent barrier coverage [1] [14] [15] considered intrusion detection in a barrier area, which is quite different from traditional 2D plane coverage. All these works are, however, based on the 2D ideal plane and no complex surface in 3D space has yet been considered.

III. Assumptions, Models and Problem Statement

In this section, our sensor, surface and distribution models are described. This is followed by a formal statement of the surface coverage problem in WSNs and a brief summary of integral geometry and the Poisson point process.

A. Sensor models

We assume that all sensors have the same sensing radius r in 3D Euclid space. They are statically deployed and stationary after deployment. A point is said to be *covered* by a sensor if it is located within the sensing area of the sensor. The sensor network is thus partitioned into two regions, the *covered region* which is covered by at least one sensor; and, *the uncovered region*, which is the complement of the covered region.

B. Surface models

We assume the FoI is convex and the surface can be expressed as a single valued function $z = f(x, y)$ in a Cartesian coordinate system which is considered the *reference system* for this surface. A surface is a *plane* if and only if the function is $z = c$ where c is a constant. A surface is a *slant* if and only if the function is $z = ax + by + c$ where a, b, c are constants. A sensor is said to be placed on the surface if its position lies on the surface. In this paper, we consider the FoI to be finite; the edge effect will be taken into account in all our calculations.

C. Sensor distribution models

Definition III.1. *The* Z-projection *of a point in 3D space is its projection point along the Z axis on the xOy plane of the reference system, i.e., if the Cartesian coordinates of a point is (x, y, z), then the coordinates of its projection is $(x, y, 0)$. The* Z-projection *of a set in 3D space is a planar point set of xOy plane which contains all the Z-projection points in the set.*

For stochastic deployment we consider two sensor distribution models. One is the *space surface Poisson point process model (SP3)* and the other is the *planar surface Poisson point process model (PP3)*.

- SP3 is described as $p_m = \frac{(\rho F)^m}{m!} e^{-\rho F}$ when sensors are deployed by humans or vehicles running on the surface.
- PP3 is described as $p_m = \frac{(\rho F')^m}{m!} e^{-\rho F'}$ when sensors are deployed by aircraft.

In the above distribution models, p_m is the probability that there are exactly m sensors on a FoI, where F is the area of the FoI, and F' is the projective area of the FoI. It can be seen that both models agree with the traditional distribution model (i.e. Poisson Point Process) when the surface is an ideal plane.

D. Problem statements

Definition III.2. *Let $z = f(x, y)$ be a surface S in 3D space. Let $\parallel S \parallel$ be the area of the surface S. The function $g : S \rightarrow 2^S$ is a function defined on the surface. Its value is the point set which is covered by sensor when the independent variable is the position of the sensor. The function $g^* : 2^S \rightarrow 2^S$ is a set function defined as: $C \subseteq S$, $g^*(C) = \bigcup_{t \in C} g(t)$.*

Definition III.3. The coverage ratio *is defined as: Given a point set $P(P \subseteq S)$, the coverage ratio f_c is a real value expressed as $f_c = \frac{\|g^*(P)\|}{\|S\|}$.*

Because f_c depends on the deployment of sensors P, we focus on the expected value of the coverage ratio $E(f_c)$ when P follows some distribution.

Definition III.4. *A feasible solution to the coverage problem is defined as a point set C that satisfies $C \subseteq S, g^*(C) \supseteq S$.* The optimum surface coverage problem (OSCP) *is defined as: $minimize|C|, C$ is a feasible solution.*

E. Integral geometry and Poisson Point Process

Lemma III.1. *The Z-projection of a convex set $\mathcal{C}$ in 3D space is a planar convex set.*

Definition III.5. *Parallel convex sets. The parallel set $\mathcal{K}_r$, in the distance r of a convex set $\mathcal{K}$ is the union of all closed circular disks of radius r, the centers of which are points of $\mathcal{K}$. The boundary $\partial\mathcal{K}_r$, is called the outer parallel curve of $\partial\mathcal{K}$ in the distance r.*

Lemma III.2. *Let the area of the convex set $\mathcal{K}$ be F and perimeter of the convex set be L. Then the area F_r and perimeter L_r of the parallel convex set $\mathcal{K}_r$ is:*

$$F_r = F + Lr + \pi r^2 \tag{1}$$

$$L_r = L + 2\pi r \tag{2}$$

Definition III.6. *Poisson Point Process. Let $\mathcal{D}_0$, $\mathcal{D}$ be two domains of the plane such that $\mathcal{D} \subseteq \mathcal{D}_0$. Let F_0, F be the areas of $\mathcal{D}_0$, $\mathcal{D}$. According to the density $dP = dx \wedge dy$, the probability that a random point of $\mathcal{D}_0$ lies in D is F/F_0. If there are n points chosen at random in $\mathcal{D}_0$, the probability that exactly m of them lie in $\mathcal{D}$ is a* binomial distribution

$$p_m = \binom{n}{m} \left(\frac{F}{F_0}\right)^m \left(1 - \frac{F}{F_0}\right)^{n-m} \tag{3}$$

If $\mathcal{D}_0$ expands to the whole plane and both n, $F_0 \rightarrow \infty$ in such a way that $\frac{n}{F_0} \rightarrow \rho$, which is a positive constant, we get

$$\lim p_m = \frac{(\rho F)^m}{m!} e^{-\rho F} \tag{4}$$

The right-hand side of (4) is the probability function of the Poisson distribution*; it depends only on the product ρF, which is called the parameter of the distribution. This probability model for points in the plane is said to be a* homogeneous planar Poisson point process of intensity *ρ. In the following, we simplify it as* Poisson Point Process*.*

Lemma III.3. *Let $\mathcal{A}_0$ be a fixed convex set of area F_0 and perimeter L_0, and let $\mathcal{A}_1$ be a convex set of area F_1 and perimeter L_1. $\mathcal{A}_1$ is randomly dropped in the plane in such a way that it intersects with $\mathcal{A}_0$. The probability that a randomly selected point $P \in \mathcal{A}_0$ is covered by $\mathcal{A}_1$ is given by:*

$$p(P \in \mathcal{A}_1) = \frac{2\pi F_1}{2\pi(F_0 + F_1) + L_0 L_1} \tag{5}$$

Lemma III.4. *Let $\mathcal{A}_0$ and $\mathcal{A}_1$ be two fixed convex set of area F_0, F_1 and perimeter L_0, L_1, and $\mathcal{A}_0 \subseteq \mathcal{A}_1$. Let $\mathcal{A}_2$ be a convex set of area F_2 and perimeter L_2, randomly dropped in the plane in such a way that it intersects with $\mathcal{A}_1$. The probability that it intersects with $\mathcal{A}_0$ is given by:*

$$p(\mathcal{A}_0 \bigcap \mathcal{A}_2 \neq \emptyset \mid \mathcal{A}_1 \bigcap \mathcal{A}_2 \neq \emptyset) = \frac{2\pi(F_0 + F_2) + L_0 L_2}{2\pi(F_1 + F_2) + L_1 L_2} \tag{6}$$

For a more detailed proof, please refer to the book [19].

IV. Expected Coverage Ratio under Stochastic Distribution Models

A. Expected coverage ratio on a plane

Theorem IV.1. *Let $\mathcal{A}_f$ be a FoI of area F_f and perimeter L_f on a plane, and let N sensors with sensing radius r and sensing area $\mathcal{A}_i$ be stochastically placed on the plane in such a way that it intersects with $\mathcal{A}_f$ according to PP3 model or SP3 model. The probability that a randomly chosen point P of $\mathcal{A}_f$ is covered by some sensors is given by:*

$$p(P \in \mathcal{A}_i) = 1 - \left(1 - \frac{2\pi^2 r^2}{2\pi\left(\pi r^2 + F_f\right) + 2\pi r L_f}\right)^N \tag{7}$$

Corollary IV.1. *Let $\mathcal{A}_f$ be a FoI of area F_f and perimeter L_f on a plane. Let the distribution of the sensors with sensing radius r be PP3 model or SP3 model with intensity λ. The expected coverage ratio $E(f_c)$ of the FoI $\mathcal{A}_f$ is:*

$$1 - \left(1 - \frac{2\pi^2 r^2}{2\pi\left(\pi r^2 + F_f\right) + 2\pi r L_f}\right)^{\lambda\left(F_f + L_f r + \pi r^2\right)} \tag{8}$$

Proof: By combining Lemma III.2 and Theorem IV.1, it can be immediately obtained. ■

B. Expected coverage ratio on a slant

Theorem IV.2. *Let $\mathcal{A}_f$ be a FoI of area F_f and perimeter L_f on a slant. Let the distribution of the sensors with sensing radius r be SP3 model with intensity λ. The expected coverage ratio $E(f_c)$ of the FoI $\mathcal{A}_f$ is:*

$$1 - \left(1 - \frac{2\pi^2 r^2}{2\pi\left(\pi r^2 + F_f\right) + 2\pi r L_f}\right)^{\lambda\left(F_f + L_f r + \pi r^2\right)} \tag{9}$$

Proof: For SP3, it is similar to PP3 after some rotation of the reference system. So, it can be immediately obtained from the Corollary IV.1. ■

Lemma IV.1. *For any slant in reference system, if its included angle with the xOy plane is θ, the ratio between the area of*

any convex area and its Z-projection convex area is a constant. Its value equals to $\sec\theta$.

Theorem IV.3. *Let $\mathcal{A}_f$ be a FoI of area F_f and perimeter L_f on a slant whose equation can be expressed as $z = ax+by+c$. Let the distribution of the sensors with sensing radius r be PP3 model with intensity λ. The expected coverage ratio $E(f_c)$ of the FoI $\mathcal{A}_f$ is:*

$$1-\left(1-\frac{2\pi^2r^2}{2\pi\left(\pi r^2+F_f\right)+2\pi rL_f}\right)^{\lambda\cos\theta\left(F_f+L_fr+\pi r^2\right)} \tag{10}$$

where

$$\theta=\arccos\left(\frac{1}{\sqrt{a^2+b^2+1}}\right)\qquad 0\le\theta<\frac{\pi}{2} \tag{11}$$

Proof: The PP3 model with intensity λ can be considered as SP3 with intensity $\lambda\cos\theta$. By combining Corollary IV.1 and Lemma IV.1, it can be immediately obtained. ■

C. Results for general complex surface

We simplify the complex surface into many small triangles as it pertains to 2D ideal planes to a complex surface. From this, we are able to obtain an approximate value for the coverage ratio when sensors are stochastically deployed. Let $\mathcal{A}_f$ be the FoI with area F_f and perimeter L_f. We divide $\mathcal{A}_f$ into many small pieces of triangle $\mathcal{A}_i$, with area F_i and perimeter L_i, where i varies from 1 to n. We model the sensing area of the sensor as a circle with radius r. Let $\mathcal{A}_0$ be the sensing region of the sensor with area F_0 and perimeter L_0. This is reasonable when variations in the surface are not significant within the sensing area of a single sensor. As mentioned, we discuss two sensor distribution models separately.

Theorem IV.4. *(for space surface Poisson Point Process model (SP3)) Let the sensor distribution be SP3 on a general complex surface. The probability that a randomly chosen point P of $\mathcal{A}_f$ is covered by the sensor is given by:*

$$p(P\in\mathcal{A}_0)=\frac{2\pi^2r^2}{2\pi\left(\pi r^2+F_f\right)+2\pi rL_f} \tag{12}$$

Proof:

$$\begin{aligned} & p(P\in\mathcal{A}_0)\\ =\ & \sum_i p(P\in\mathcal{A}_0\mid P\in\mathcal{A}_i)p(P\in\mathcal{A}_i)\\ =\ & \sum_i \frac{F_i}{F_f}\frac{2\pi F_0}{2\pi\left(F_0+F_i\right)+L_0L_i}\frac{2\pi\left(F_0+F_i\right)+L_0L_i}{2\pi\left(F_0+F_f\right)+L_0L_f}\\ =\ & \frac{2\pi^2r^2}{2\pi\left(\pi r^2+F_f\right)+2\pi rL_f} \end{aligned} \tag{13}$$

■

Corollary IV.2. *Let the sensor distribution be SP3 with intensity λ on a general complex surface, the expected coverage ratio $E(f_c)$ of a FoI $\mathcal{A}_f$ with area F_f and perimeter L_f is:*

$$1-\left(1-\frac{2\pi^2r^2}{2\pi\left(\pi r^2+F_f\right)+2\pi rL_f}\right)^{\lambda\left(F_f+L_fr+\pi r^2\right)} \tag{14}$$

Proof: Combining Lemma III.2 and Theorem IV.4, it can be immediately obtained. ■

Theorem IV.5. *(for planar surface Poisson Point Process model (PP3)) Let the sensor distribution be PP3 on a general complex surface. The probability that a randomly chosen point P of $\mathcal{A}_f$ is covered by the sensor is given by:*

$$\sum_i \frac{F_i}{F_f}\frac{2\pi^2r^2}{2\pi\left(\pi r^2+F_i\right)+2\pi rL_i}\frac{\left(F_i+L_ir+\pi r^2\right)\cos\theta_i}{F_f^{'}+L_fr+\pi r^2} \tag{15}$$

where θ_i is the included angle between $\mathcal{A}_i$ plane and xOy plane of the reference system and $F_f^{'}$ is the area of Z-projection of $\mathcal{A}_f$.

Proof:

$$\begin{aligned} p(P\in\mathcal{A}_0) &= \sum_i p(P\in\mathcal{A}_0\mid P\in\mathcal{A}_i)p(P\in\mathcal{A}_i)\\ &= \sum_i p(P\in\mathcal{A}_i)\\ &\quad p(P\in\mathcal{A}_0\mid P\in\mathcal{A}_i,\mathcal{A}_i\cap\mathcal{A}_0\neq\emptyset)\\ &\quad p(\mathcal{A}_i\cap\mathcal{A}_0\neq\emptyset)\\ &= \sum_i \frac{F_i}{F_f}\frac{2\pi^2r^2}{2\pi\left(\pi r^2+F_i\right)+2\pi rL_i}\\ &\quad \frac{\left(F_i+L_ir+\pi r^2\right)\cos\theta_i}{F_f^{'}+L_fr+\pi r^2} \end{aligned} \tag{16}$$

■

Corollary IV.3. *Let the sensor distribution be PP3 with intensity λ on a general complex surface; the expected coverage ratio $E(f_c)$ of a FoI $\mathcal{A}_f$ with area F_f and perimeter L_f is:*

$$\begin{aligned} E(f_c) &= 1-(1-\sum_i \frac{F_i}{F_f}\frac{2\pi^2r^2}{2\pi\left(\pi r^2+F_i\right)+2\pi rL_i}\\ &\quad \frac{\left(F_i+L_ir+\pi r^2\right)\cos\theta_i}{F_f^{'}+L_fr+\pi r^2})^{\lambda\left(F_f^{'}+L_fr+\pi r^2\right)} \end{aligned} \tag{17}$$

Proof: By combining Lemma III.2 and Theorem IV.3, it can be immediately obtained. ■

We can easily verify that the results of PP3 and SP3 are the same, and match precisely the previous result when the surface is an ideal plane, i.e. $\theta_i=0$, $F_f^{'}=F_f=\sum_i F_i$.

V. Deterministic Deployment Problem

The original optimum surface coverage problem is a difficult continuous problem; and so, we convert it to a discrete problem and then relate those results back to the original continuous problem. We prove the hardness of the problem and propose three algorithms offering approximate solutions.

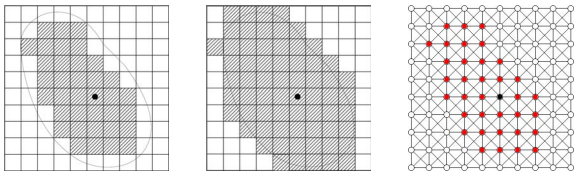

(a) (b) (c)

Fig. 2. The concept of a). inner-projection, b). outer-projection, c). topology graph.

Definition V.1. *A* Partition *is a set defined on a surface S: $P = \{S_1, S_2, \ldots, S_k\}$ which satisfies: $S_i \subseteq S (i = 1 \ldots k)$, $S_i \bigcap_{i \neq j} S_j = \emptyset$, and $\bigcup_{i=1}^{k} S_i = S$. Let $\mathcal{P}$ be the set of all the partitions. Use $Gran(P) = \max_{i=1\ldots k}\{\| S_i \|\}$ to denote granularity of partition P. The relation $\preceq$ is a partial semi-order relation in $\mathcal{P} \times \mathcal{P}$: $P_i \preceq P_j$ if and only if P_j is a finer partition than P_i. The function $h : P \rightarrow 2^P$ is a function defined on partition P. Its value is a partition set that is covered by a sensor, where the independent variable is the position of the sensor. The function $h^* : 2^P \rightarrow 2^P$ is a set function defined as: $L \subseteq P$, $h^*(L) = \bigcup_{t \in L} h(t)$.*

Definition V.2. *The* topology graph of partition P *is a graph $G(V, E)$, where a vertex v_i corresponds to S_i in partition P. An edge is added between vertices v_i and v_j if S_i and S_j are neighbors to each other by sharing their border or a common point. Fig.2(c) shows the corresponding topology graph of Fig.2(a). The distance between two pieces in a partition is defined as the length of the shortest path between the corresponding vertices. For a sensor positioned at any piece S_i, its sensing radius R is defined as the longest distance from v_i to any other vertex within its sensing area; whereas, its sensing diameter D is defined as the longest distance between any two vertices within its sensing area.*

Definition V.3. A feasible solution to the partition coverage problem *is defined as a set L satisfying $L \subseteq P$ and $h^*(L) \supseteq P$. The* Optimum Partition Coverage Problem (OPCP) *is defined as: minimize $|L|$, L is a feasible solution.*

To solve the OSCP, we have converted the problem from its original continuous form to a discrete one. If function g in the continuous version and function h in the discrete one are correlated, we can establish a relationship between their corresponding solutions as specified in the following lemmas.

Lemma V.1. *For every $S_i \in$ partition P, if there exists a point k in S_i to satisfy $g(k) \supseteq h(S_i)$, any feasible solutions to the discrete version of the problem will be a feasible solution to the continuous version; For any point k in S_i, if $h(S_i) \supseteq g(k)$, any feasible solutions to the continuous version of the problem will be a feasible solution to the discrete version.*

In fact, due to the impact of the surface, the coverage area of a sensor is no longer a unit disk. The function g is determined by the characteristic of the surface. For the discrete problem, there are two mechanisms to deal with the boundary: inner-projection and outer-projection. The values of an inner-projection function are all the pieces located within the coverage area, i.e., $g(k) \supseteq h(S_i)$. On the other hand, the values of an outer-projection function include that of inner-projection plus all the pieces located at the boundary, i.e. $h(S_i) \supseteq g(k)$. Figs 2(a) and 2(b) show the instances of the inner-projection and outer-projection for the same function g. In order to satisfy the first part of Lemma V.1, we focus on the inner-projection function from now on to ensure that our results for the discrete problem are applicable to the continuous problem.

Lemma V.2. *Let S_{opt} be the solution to the OSCP, P_{opt} be the solution to the OPCP under partition P, and function h be an inner-projection of function g in the OSCP. Let $P^1, P^2, \ldots, P^i, \ldots$ be a sequence of partitions with $P^i \preceq P^{i+1}$ and $\lim_{i \rightarrow \infty} Gran(P^i) = 0$. We have P^i_{opt} is monotonically decreasing as i increases and $\lim_{i \rightarrow \infty} P^i_{opt} = S_{opt}$.*

The above two lemmas guarantee that when the partition is fine enough, the result of the OPCP can approximate the result of the OSCP precisely. To show the hardness of the OPCP, we prove that a special case of the OPCP, called *Optimum Rectangular Grid Coverage (ORGC)* problem, is NP-complete. The ORGC problem limits the shape of the sensing area and the shape of the partition in the original partition coverage problem. Since the ORGC problem is a special case of OPCP, the latter is also NP-complete.

A. The hardness of the ORGC problem

Definition V.4. The Optimum Rectangular Grid Coverage (ORGC) *problem is defined as: we consider an $N \times N$ grid $\mathcal{G}$, where each pane $E_{(i,j)} \in \mathcal{G}$ is associated with four numbers to specify its coverage rectangle $\mathcal{O}_{(i,j)}$. The ORGC problem is to find a subset $\mathcal{G}'$ that minmizes $|\mathcal{G}'|$ while satisfying: $\{\bigcup_{E_{(i,j)} \in \mathcal{G}'} \mathcal{O}_{(i,j)}\} \supseteq \mathcal{G}$.*

Definition V.5. The k determination of the ORGC problem: *given a grid $\mathcal{G}$, determine if there exists a cover set $\mathcal{G}' \subseteq \mathcal{G}$ satisfying $|\mathcal{G}'| = k$ and $\{\bigcup_{E_{(i,j)} \in \mathcal{G}'} \mathcal{O}_{(i,j)}\} \supseteq \mathcal{G}$.*

If pane $E_{(x,y)}$ associated with (a_1, a_2, a_3, a_4) is selected, it can cover $\mathcal{O}_{(x,y)}$, a rectangular area from pane $E_{(x-a_1, y+a_2)}$ to pane $E_{(x+a_3, y-a_4)}$. For example, if we have pane $E_{(1,1)}$ associated with $(0, 1, 1, 1)$, it can cover $\mathcal{O}_{(1,1)}$, a rectangle from pane $E_{(1,2)}$ to pane $E_{(2,0)}$ as shown in Fig.4(a).
Here are symbols to be used in the following theorem:

- N: length of the grid.
- m: number of clauses in an instance of P3SAT.
- n: number of variables in an instance of P3SAT.
- t_i: number of appearances of the ith variable ($1 \leq i \leq n$).
- e: number of edges between clauses and literals; calculated by $\sum_{i=1}^{n} t_i$.
- p_j: number of panes on the jth path ($1 \leq j \leq e$).

Theorem V.1. *ORGC problem is NP-complete.*

Proof: Planar 3SAT (P3SAT) is 3SAT restricted to formulae B such that $G(B)$ is planar. P3SAT is NP-complete[20]. We divide the procedure of reducing from P3SAT into two

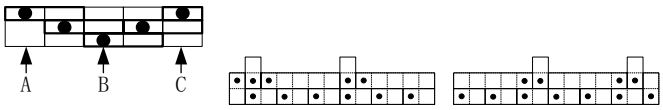

(a) clause gadget. (b) variable gadget1. (c) variable gadget2.

Fig. 3. The concepts of clause gadget and variable gadget

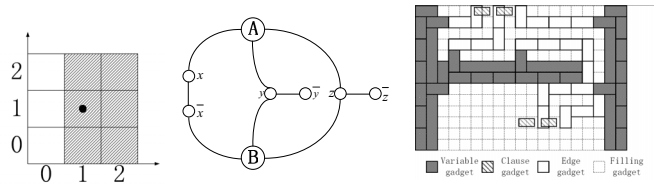

(a) (b) (c)

Fig. 4. The concept of a). covered region in ORGC, b). the instance of P3SAT, c). its converted ORGC instance.

steps. Firstly, we show that there is a polynomial time computable function f which converts an instance in P3SAT to an instance in ORGC. Secondly, we prove that:

$$w \in P3SAT \Longleftrightarrow f(w) \in ORGC \tag{18}$$

where w is an instance in P3SAT. Next, we describe the polynomial time computable function f. Fig.4(b) shows an instance of formulae $(x \vee y \vee z) \wedge (\bar{x} \vee y \vee z)$. It is made up of three basic elements: clause nodes, variable nodes, and edges. We convert them separately into gadgets according to the following rules. We select a sufficiently large N to guarantee that any two gadgets will not overlap and that their edges can be substituted by rectilinear paths. The planarity of P3SAT guarantees that no two paths will crossover. For convenience, we use a rectangular area and a point instead of the four numbers to indicate the area to be covered.

For each clause, we convert it to a gadget as shown in Fig.3(a). A, B, C are three connection points which must be connected with the path from the literal occurring in the clause.

For variable i which occurs t_i times, we convert it to a gadget shown in Fig.3(b) and 3(c) with length of $(6t_i + 1)$.

For the paths, we convert them to a series of 1×2 dominos. If the length of a path is odd, we add a 1×3 domino to guarantee that the total dominos used to propagate satisfiable assignment is $\lfloor \frac{p_j}{2} \rfloor$.

We use 1×1 dominos to fill other blank areas. The time complexity needed to convert the planar graph to a rectangular grid coverage problem is polynomial. The corresponding instance of ORGC is shown in Fig.4(c).

For the clause gadget, we can easily verify the following properties: if any true assignment is not propagated to a clause gadget (none of three connection points is covered), it must be covered by three dominoes. Otherwise, it can be covered by two dominoes. Even if all three variables are true, it still needs two dominoes to cover the area.

For the variable gadget, the first case in Fig.3(b) means X_i is assigned a true value; the second case in Fig.3(c) means X_i is assigned a false value. We can easily verify the following properties: for a gadget of length $(6t_i + 1)$ (means total $2 \times (6t_i + 1)$ panes), it needs at least $(5t_i + 1)$ dominoes to cover the full area. If each occurrence of a literal is consistent, we can use $(5t_i + 1)$ dominoes to fully cover the area. Otherwise, more than $(5t_i + 1)$ dominoes are required to fully cover the area.

For the paths, whatever its length, we can use $\sum_{j=1}^{e} \lfloor \frac{p_j}{2} \rfloor$ dominoes to propagate the satisfiable assignment.

Based on the above properties, for an instance of P3SAT, there must be a consistent assignment to all the variables that satisfy all the clauses. The total number of dominoes is: $R = N^2 - [\sum_{i=1}^{n}(7t_i + 1)] - 3m - \sum_{j=1}^{e} \lceil \frac{p_j}{2} \rceil$. Next, if a grid can be covered by selecting R panes, the minimum coverage of every gadget is achieved. We know that each clause is covered by two dominoes. It implies that there must be no fewer than one satisfied assignment. So the corresponding instance is satisfiable and the next lemma can be given. ■

Lemma V.3. *An instance of P3SAT is satisfiable if and only if its corresponding grid can be R coverage.*

B. Approximation algorithms for solving the Optimum Partition Coverage Problem (OPCP)

Since the OPCP is NP-complete, we propose three algorithms to solve it approximately. Algorithm 1 is a greedy algorithm. It selects a position that can increase the covered region the most.

Algorithm 1: Approximation Algorithm for OPCP

Input : Partition $\mathcal{P}$, function h of every pieces S_i
Output: A subset $\mathcal{P}'$ of $\mathcal{P}$

$\mathcal{P}' \leftarrow \emptyset$; $\mathcal{C} \leftarrow \emptyset$;
while $\mathcal{C} \not\supseteq \mathcal{P}$ **do**
  $m \leftarrow 0, x \leftarrow 0$;
  for *every* S_i *in* $\mathcal{P} - \mathcal{P}'$ **do**
    if $|h(\mathcal{S}_i) - \mathcal{C}| > m$ **then**
      $m \leftarrow |h(\mathcal{S}_i) - \mathcal{C}|; x \leftarrow i$;
    end
  end
  $\mathcal{P}' \leftarrow \mathcal{P}' \cup \{S_x\}$; $\mathcal{C} \leftarrow \mathcal{C} \cup h(\mathcal{S}_x)$;
end

Theorem V.2. *Algorithm 1 is an $O(|\mathcal{P}|^2)$ time $\log(|\mathcal{P}|)$-approximation algorithm.*

Proof: Let $\mathcal{C}_i$ denote the partition set $\mathcal{C}$ after the ith turn selection of the algorithm 1. Let $\mathcal{NC}_i$ denote the set of newly covered panes in turn i. Actually, $\mathcal{NC}_i = h(\mathcal{S}_i) - \mathcal{C}_{i-1}$, where $\mathcal{S}_i$ is the selected piece of turn i. $|\mathcal{P}|$ is the total pieces of the partition $\mathcal{P}$. $\mathcal{P}_{opt}$ is the optimal selection of panes, i.e. the optimal solution to OPCP problem. Let $\mathcal{P}'_{opt}$ be the current optimal solution after some pieces has been covered. Obviously, $|\mathcal{P}'_{opt}| \leq |\mathcal{P}_{opt}|$. Then we have:

$$\frac{1}{|\mathcal{NC}_i|} \quad \leq \quad \frac{|\mathcal{P}'_{opt}|}{|\mathcal{P}| - |\mathcal{C}_{i-1}|} \leq \frac{|\mathcal{P}_{opt}|}{|\mathcal{P}| - |\mathcal{C}_{i-1}|} \tag{19}$$

Finally, for our solution k, we have

$$\begin{aligned} k &= \sum_{i=1}^{k} |\mathcal{NC}_i| \frac{1}{|\mathcal{NC}_i|} \\ &\leq \frac{|\mathcal{P}_{opt}|}{|\mathcal{P}|} + \frac{|\mathcal{P}_{opt}|}{|\mathcal{P}|-1} + \ldots + \frac{|\mathcal{P}_{opt}|}{1} \\ &= |\mathcal{P}_{opt}| \sum_{i=1}^{|\mathcal{P}|} \frac{1}{i} \end{aligned} \quad (20)$$

Since $\sum_{i=1}^{N} \frac{1}{i}$ is the harmonic series, its value is $\ln(n+1)+r$ where r is the Euler constant. Then we have:

$$k \leq |\mathcal{P}_{opt}|(\ln(|\mathcal{P}|+1)+r) \leq |\mathcal{P}_{opt}|(\ln(|\mathcal{P}|)+1) \quad (21)$$

From this equation, we derive our conclusion. ■

Actually, if we assume the diameter of the sensing area is D as defined in definition V.2, then we can make use of the "shifting strategy" proposed in paper[21] to develop an polynomial-time approximation scheme(PTAS) algorithm to solve it. The approximation ratio can be $(1+\frac{1}{\epsilon})^2$. Since it is based on divide-and-conquer idea, it can be easily implemented in a distributed manner.

The main idea is to divide the FoI into vertical strips of width D. These strips are then considered in groups of l consecutive strips resulting in strips of width $l \times D$ each. For any fixed division into strips of width D, there are l different ways of partitioning FoI into strips of width $l \times D$. These partitions can be ordered such that each can be derived from the previous one by shifting it to the right over distance D. We use the same method to solve the subproblem and output the union of all positions. For l different shifting partitions, we select the optimum result as the final result. We give the framework of the algorithm in the following:

Algorithm 2: Approximation Algorithm for OPCP

Input : Partition $\mathcal{P}$, the function h of every pieces S_i
Output: A subset $\mathcal{P}'$ of $\mathcal{P}$

Divide $\mathcal{P}$ into vertical strips to generate l shifting partitions $P^1, P^2, \ldots, P^l$;
for *each shifting partition* P^i **do**
  for *each strip group* $P^i_j \in P^i$ **do**
    Divide P^i_j into horizontal strips to generate l shifting partitions $SP^1, SP^2, \ldots, SP^l$;
    for *each shifting partition* SP^u **do**
      for *each strip group* $SP^u_v \in SP^u$ **do**
        Using brute-force algorithm to solve the subproblem SP^u_v and let the result be R^u_v;
      end
      $R^u \leftarrow \bigcup_{v=1}^{\lceil \frac{m}{l \times D} \rceil} R^u_v$;
    end
    $R^i_j \leftarrow \min_{|R^u|} R^u$;
  end
  $R^i \leftarrow \bigcup_{j=1}^{\lceil \frac{n}{l \times D} \rceil} R^i_j$;
end
$\mathcal{P}' \leftarrow \min_{|R^i|} R^i$;

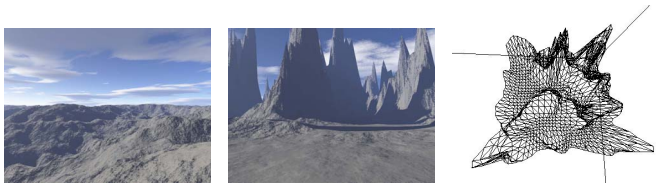

(a) (b) (c)

Fig. 5. a). Terrain1 (Glaciation=0). b). Terrain2 (Glaciation=100). c). Terrain after triangularization.

Theorem V.3. *Algorithm 2(a) is an* $O(\frac{|\mathcal{P}|}{D^2} \times 2^{l^2 D^2})$ *time* $(1+\frac{1}{l})^2$*-approximation algorithm.*

Proof: Due to the limitation of space, details of the proof is omitted. The proof is similar to [21]. ■

Although the performance ratio looks fine, it may be not practical in real environments because even $l=1$ is a big cost since D is often larger than five. We sacrifice some accuracy to reduce the cost of calculation. This brings us to algorithm 2(b). It mixes the core idea in algorithm 1 and algorithm 2(a) and simply uses the greedy algorithm described in algorithm 1 instead of the brute-force algorithm in algorithm 2(a). It can still be implemented in a distributed manner. We call it algorithm 2(b).

Lemma V.4. (shifting lemma) *Let* A *be a local algorithm with the approximation ratio* r_A *and* l *be the shifting parameter then the approximation ratio of the shifting algorithm is* $r_{S_A} \leq r_A(1+\frac{1}{l})$.

From the shifting lemma given in [21] and theorem V.2, we can easily derive the following theorem:

Theorem V.4. *Algorithm 2(b) is an* $O(|\mathcal{P}|l^4D^2)$ *time* $\log(l^2D^2) \times (1+\frac{1}{l})^2$*-approximation algorithm.*

VI. Performance Evaluation

The main purpose of our evaluation is to: (a) point out the limitation of the traditional methods. (b) verify our derived results. (c) make comparisons of the three proposed algorithms in a comprehensive manner.

We use Terragen[22], a professional terrain-generating tool to simulate surface, and the widely-used "Ridged Perlin Noise" to generate a natural, ridged landscape. Fig.5(a) and Fig.5(b) show the impact of different parameters on the terrain. As a lower Glaciation will generate a flatter terrain and vice versa. Glaciation is used as a measurement of this characteristic of the terrain. We use triangularization to partition a surface. Fig.5(c) depicts surface triangularization.

There are several methods used to cover the FoI on an ideal plane. The most widely used is the triangle pattern [23]. Furthermore, it can provide 6-connectivity while $\frac{r_c}{r_s} \geq \sqrt{3}$. Thus, we take these as representative patterns for performance evaluation. Six different terrains are generated and evaluated with different glaciations and we treat them as ideal planes when we deploy sensors on them. Finally, we calculate the coverage ratio. The size of the FoI is set to $1920 \times 1920 m^2$.

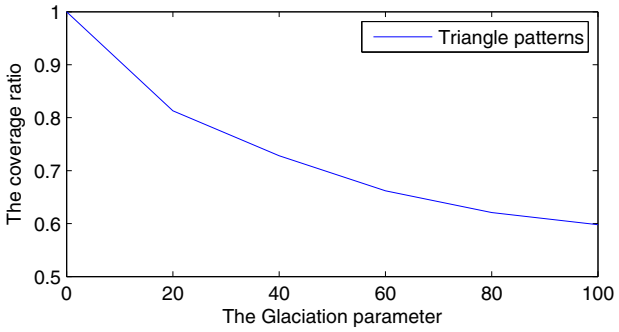

Fig. 6. The relationship between coverage ratio and surface parameter.

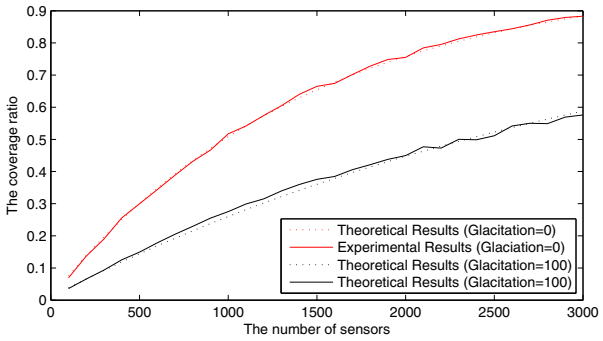

Fig. 7. The expected coverage ratio(Theoretical value vs. experimental value).

The height ranges are from $300m$ to $2000m$ and the sensing radius is $30m$.

Fig.6 presents the performance of previous triangle patterns. When $glaciation = 0$, the coverage ratio is 1. The coverage ratio drops quickly when the parameter increases and it can drop to about 60%. So, the previous triangle patterns do not work well on a complex surface. We need to find new methods to cover the complex surface.

Fig.7 shows that our theoretical results match the simulation results precisely. We stochastically deploy some sensors and calculate the coverage ratio.

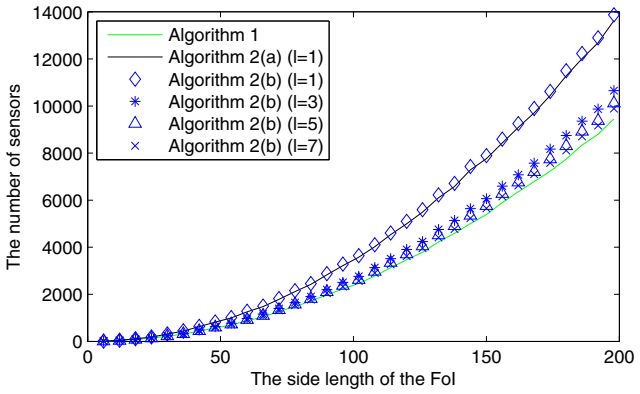

Fig. 8. The results of the different algorithms when $D = 3$.

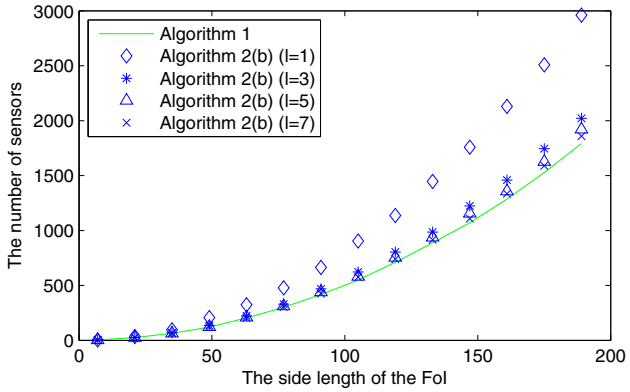

Fig. 9. The results of the different algorithms when $D = 7$.

Fig.8 and Fig.9 compare the results of the three algorithms. We use a square partition in our experiment because the terrain file is a dot matrix and can be easily converted to a square partition. The FoI is a $N \times N$ grid, where N is the distance measured by partitions. The X-axis is the side length of the FoI and the Y-axis means how many sensors are needed to have a complete coverage of the FoI. Surprisingly, the performance of the simple greedy algorithm is best. Algorithm 2(a) has the best theoretical performance bound when l is large enough. Unfortunately, the time complexity is exponential as l increases. And so, it can only be executed effectively when $l = 1$ and $D \leq 5$. However, the little D implicates that the size of the partition is large. We must guarantee that the partition is detailed enough to get a precise solution to the original OSCP as stated in lemma V.2. In Fig.8, D is set to 3 only because we want to compare algorithm 2(a) with other algorithms.

Fig.9 compares the three algorithms when $D = 7$. The performance of algorithm 1 is still the best. Note that algorithm 2(a) and algorithm 2(b) can be implemented in a distributed manner, and we propose algorithm 2(b) because the calculation cost of algorithm 2(a) is too large.

The results tell us that algorithm 1 is the best choice. Although its theoretical performance bound is not very acceptable, its average approximation ratio is precise enough.

VII. Discussions

In this section, we discuss some practical issues.

- *Surface is not a single-valued function.* Note that our solution only depends on a partition of the surface. If we have proper expressions of the surface when it is not a single-valued function, we can partition it and our solution can still be applied.
- *The errors between a smooth surface and a surface with triangles.* Due to discrepancy between a smooth surface and a triangulated surface, unavoidable errors that occur when converting a smooth surface into a triangulated one are minimized when the triangles are small. Because geographic information systems (GIS) provide data in a dot matrix, accuracy is lost in this data storage system, and not in the calculation process.

- *Relationship between surface parameter and coverage ratio.* After a survey of the current surface parameters in the GIS, we have not found any relative parameters. The impact on coverage ratio is the ratio of the area to the projective area. In general, a terrain with more mountains and densely populated with mountains will have a relatively poor coverage ratio.
- *The problem of connectivity.* If $\frac{r_c}{r_s} \geq 2$, the full coverage implicates connectivity [24]. If $\frac{r_c}{r_s} \leq 2$, previous research proposes different coverage patterns to solve this problem on an ideal plane [2]. For surface coverage, it remains an open problem.

VIII. Conclusions and Future Work

We have proposed a new model for the coverage problem called surface coverage to better capture real world application challenges. Two problems pertaining to surface coverage were in focus: the expected coverage ratio with stochastic deployment and the optimal deployment strategy with planned deployment. Comprehensive simulation experiments show that though the performance bound of the greedy algorithm is not the best, it often outperforms the other two algorithms. To our best knowledge, this is the first attempt to describe and resolve the surface coverage problem in WSNs.

Future research can be carried out following many directions. We assume that the FoI is convex. Real world scenarios require a methodology for $FoIs$ of greater complexity. Also, our research is restricted to the PP3 and SP3 sensor distribution model for random deployment, but many others can and should be explored. Furthermore, our research considers only static/homogenous sensors, which may be mobile/heterogeneous in practice. Communication connectivity and multiple coverage are also topics worthy of further study.

Acknowledgements

This research was partially supported by NSF of China under grant No. 60773091, 973 Program of China under grant No. 2006CB303000, 863 Program of China under grant No. 2006AA01Z247, Hong Kong RGC Grants HKUST617908 and HKBU 1/05C, the Key Project of China NSFC Grant 60533110. Our shepherd, Jin-Yi Cai, Xiang-Yang Li, Dong Xuan, Ten H. Lai, Lionel M. Ni gave us highly valuable comments to improve the paper.

References

[1] Santosh Kumar, Ten H. Lai, and Anish Arora. Barrier coverage with wireless sensors. In *MobiCom'05.*, pages 284–298, New York, NY, USA, 2005. ACM.

[2] Xiaole Bai, Dong Xuan, Ziqiu Yun, Ten H. Lai, and Weijia Jia. Complete optimal deployment patterns for full-coverage and k-connectivity (k$\leq$6) wireless sensor networks. In *MobiHoc'08.*, pages 401–410, New York, NY, USA, 2008. ACM.

[3] Chi-Fu Huang, Yu-Chee Tseng, and Li-Chu Lo. The coverage problem in three-dimensional wireless sensor networks. *IEEE GLOBECOM'04.*, 5:3182–3186 Vol.5, Nov.-3 Dec. 2004.

[4] M.K. Watfa and S. Commuri. A coverage algorithm in 3d wireless sensor networks. *Wireless Pervasive Computing, 2006 1st International Symposium on*, pages 6 pp.–, Jan. 2006.

[5] http://fiji.eecs.harvard.edu/Volcano/.

[6] S. Meguerdichian, F. Koushanfar, M. Potkonjak, and M.B. Srivastava. Coverage problems in wireless ad-hoc sensor networks. *INFOCOM 2001.*, 3:1380–1387 vol.3, 2001.

[7] K. Kar and S. Banerjee. Node placement for connected coverage in sensor networks. *Modeling and Optimization in Mobile, Ad Hoc and Wireless Networks and Workshops, 2003. WiOpt 2003. 1th International Symposium on*, pages 1–10, April 2003.

[8] Xiang-Yang Li, Peng-Jun Wan, and O. Frieder. Coverage in wireless ad hoc sensor networks. *Computers, IEEE Transactions on*, 52(6):753–763, June 2003.

[9] Xiaorui Wang, Guoliang Xing, Yuanfang Zhang, Chenyang Lu, Robert Pless, and Christopher Gill. Integrated coverage and connectivity configuration in wireless sensor networks. In *SenSys'03.*, pages 28–39, New York, NY, USA, 2003. ACM.

[10] Benyuan Liu, Peter Brass, Olivier Dousse, Philippe Nain, and Don Towsley. Mobility improves coverage of sensor networks. In *MobiHoc'05.*, pages 300–308, New York, NY, USA, 2005. ACM.

[11] M. Cardei, M.T. Thai, Yingshu Li, and Weili Wu. Energy-efficient target coverage in wireless sensor networks. *INFOCOM 2005.*, 3:1976–1984 vol. 3, March 2005.

[12] Rajagopal Iyengar, Koushik Kar, and Suman Banerjee. Low-coordination topologies for redundancy in sensor networks. In *MobiHoc'05.*, pages 332–342, New York, NY, USA, 2005. ACM.

[13] Loukas Lazos and Radha Poovendran. Stochastic coverage in heterogeneous sensor networks. *ACM Trans. Sen. Netw.*, 2(3):325–358, 2006.

[14] Ai Chen, Santosh Kumar, and Ten H. Lai. Designing localized algorithms for barrier coverage. In *MobiCom'07.*, pages 63–74, New York, NY, USA, 2007. ACM.

[15] Paul Balister, Béla Bollobas, Amites Sarkar, and Santosh Kumar. Reliable density estimates for coverage and connectivity in thin strips of finite length. In *MobiCom'07.*, pages 75–86, New York, NY, USA, 2007. ACM.

[16] Wei Wang Vikram Srinivasan and Kee-Chaing Chua. Trade-offs between mobility and density for coverage in wireless sensor networks. In *MobiCom '07.*, pages 39–50, New York, NY, USA, 2007. ACM.

[17] Y. Bejerano. Simple and efficient k-coverage verification without location information. *INFOCOM 2008.*, pages 291–295, April 2008.

[18] P. Corke, S. Hrabar, R. Peterson, D. Rus, S. Saripalli, and G. Sukhatme. Autonomous deployment and repair of a sensor network using an unmanned aerial vehicle. *Robotics and Automation, 2004. Proceedings. ICRA '04. 2004 IEEE International Conference on*, 4:3602–3608 Vol.4, 26-May 1, 2004.

[19] Luis A. SANTALO. *Integral geometry and geometric probability*. Addison-Wesley, Massachusetts (etc.), 1976.

[20] David Lichtenstein. Planar formulae and their uses. *SIAM Journal on Computing*, 11(2):329–343, 1982.

[21] Dorit S. Hochbaum and Wolfgang Maass. Approximation schemes for covering and packing problems in image processing and vlsi. *J. ACM*, 32(1):130–136, 1985.

[22] http://www.planetside.co.uk/terragen/.

[23] R. Kershner. The number of circles covering a set. *American Journal of Mathematics*, 1939.

[24] H. Zhang and J. Hou. Maintaining sensing coverage and connectivity in large sensor networks. *Ad Hoc & Sensor Wireless Networks*, 1(1-2), 2005.